Kinetic modeling of gas-phase decomposition of propane : correlation with pyrocarbon deposition

Cédric Descamps, Gerard L. Vignoles, Olivier Féron, Jerôme Lavenac, Francis Langlais

HAL Id: hal-00337420

https://hal.science/hal-00337420

Submitted on 30 Jun 2009

Kinetic modelling of gas-phase decomposition of propane : correlation with pyrocarbon deposition

Cédric Descamps, Gerard L. Vignoles*, Olivier Féron, Jérôme Lavenac, Francis Langlais
*presenting author, to whom correspondence should be addressed

Laboratoire des composites ThermoStructuraux (LCTS)
3, Allée La Boëtie- Domaine Universitaire
F 33600 PESSAC, France
Tel : (+33) 5 56 84 47 00
Fax : (+33) 5 56 84 12 25
e-mail : vinhola@lcts.u-bordeaux1.fr

Abstract :
A chemical kinetic model for gas-phase pyrolysis of propane has been set up, partially reduced, and validated against FTIR measurements in a tubular hot-wall reactor at P=2 kPa, and T = 900 to 1400 K. It confirms the notion of "maturation" from propane to lighter hydrocarbons, then to aromatic compounds and PAHs. The gas-phase composition above the substrate has been correlated to pyrocarbon deposition rates and to the deposit nanostructure. It is confirmed that the growth of the rough laminar (RL) form would be related to heavier gaseous species than for the smooth laminar (SL) form.

1   INTRODUCTION

Gas-phase pyrolysis of hydrocarbons is a key issue in many chemistry topics, among which one finds soot formation, fuel combustion, as well as diamond and pyrocarbon deposition in CVD or CVI conditions.

It has been shown since a long time that the texture or nanostructure of pyrocarbons is highly dependent on processing conditions [1,3]. It may vary from a markedly anisotropic nanostructure up to a completely isotropic form. This nanostructure is very important for the thermal quality of carbon/carbon (C/C) composites. Depending on the degree of pyrocarbon anisotropy, one may switch from a moderately conductive material (isotropic or poorly anisotropic carbon) to a very conductive material (highly anisotropic carbon) [2,3].

The conditions of interest in this study are the experimental conditions used in previous reports [4]: total pressure ranging between 0.1 and 50 kPa, temperature between 900 K and 1400 K, pure propane as gaseous precursor ; they yield only two kinds of nanostructure : Rough Laminar (LR), very anisotropic, and Smooth Laminar (SL), less anisotropic [5,6]. A subject of concern in pyrocarbon CVD is to be able to monitor experimental conditions suitable for the synthesis of either one or the other nanotexture.

Past works concerning hydrocarbon pyrolysis in various conditions [4, 7, 8] have led to the hypothesis of concurrent reaction pathways leading to different kinds of pyrocarbon. Indeed, the successive steps in hydrocarbon pyrolysis are (i) a cracking of the initial molecules into more reactive and lighter gaseous species, (ii) a recombination of these species up to the synthesis of light aromatic compounds, and (iii) an evolution of these aromatic compounds towards higher molecular weights like in a polymerization reaction. This evolution chain is called gas-phase *maturation* [8]. Subsequent evolutions depend on the experimental conditions : if a hot substrate is present, then pyrocarbon deposition occurs ; in the converse case, soot formation predominates. Concerning pyrocarbon deposition, it has been shown that the hypothesis of two parallel reaction pathways starting from the gas phase and leading respectively to SL and RL correctly accounts for the experimental results [9]. The choice between the predominance of one or the other reaction path relies on the degree of gas-phase maturation and on limitations by transport. Indeed, a more maturated gas phase leads to a rough laminar deposit. If the maturation is lesser, the deposit is smooth laminar.

On the other hand, other works [10–13] confirm the notion of gas-phase maturation which is influenced by the residence time, the surface area/reactor volume ratio, and the temperature, but associate SL pyrocarbon to the existence of heavy, aromatic compounds. The rôle of hydrogen des-

orption as a limiting factor for the deposition rate is also pointed out.

Our concern in this study is to obtain a more precise understanding of maturation effects, as well as of the possible deposition reaction pathways leading to SL and RL textures. The first point requires an accurate description of the gas-phase phenomena. Once the composition of the gas-phase above the substrate is known, it becomes possible to try to correlate it unambiguously with deposition rates and the texture of the deposits.

We present here the study of a detailed gas-phase kinetic mechanism suited to the particular case of pyrocarbon CVD/CVI from pure propane [14]. The results of this study are : (i) a partially reduced kinetic mechanism,(ii) a better knowledge of the respective importances of the different species and submechanisms,and (iii) species concentrations in a furnace for which experimental data are available for an experimental validation of the model, and a correlation with deposition rates and deposit textures.

The modeling context will be presented first, as well as the chemical model that has been used. Then, a comparison of the results with analysis of the gas phase by FTIR spectroscopy will be made, in order to provide a qualitative validation of the model. Finally, a correlation with deposition rates measurements and deposit textures data will bring us to a tentative explanation for the SL/RL transition.

2 MODEL SETUP

2.1 Modeling context

As experimental data were obtained in our laboratory on a long, narrow, tubular furnace, a home-made 1D solver suited to this geometry and flow pattern was set up, with the following hypotheses : (i) the small diameter of the furnace implies that radial effects are of negligible importance ; (ii) the weak inflow velocity and the fact that there was no carrier gas force to take multicomponent diffusion fully into account, so that the model may not be considered as a plug-flow model. Each chemical species satisfies to a conservation equation which may be written as :

$$\underbrace{\frac{\partial \rho_i}{\partial t}}_{\text{accumulation}} + \underbrace{\nabla \cdot (\rho_i \mathbf{v})}_{\text{convection}} + \underbrace{\nabla \cdot (-\sum_j \mathsf{D}_{ij} \nabla \rho_i)}_{\text{diffusion}} = M_i R_i = \underbrace{M_i \sum_k k_k \prod_j c_j^{\nu_{jk}}}_{\text{chemical reactions}} \tag{2.1}$$

A non-homogeneous temperature profile, as obtained by experimental measurements, was assumed. The resolution of total mass balance equation gives the velocity profile along the furnace:

$$\frac{\partial \rho}{\partial t} + \nabla \cdot (\rho \mathbf{v}) = 0 \tag{2.2}$$

All quantities are assumed to be radial averages. The multicomponent diffusion coefficients were approximated using the bifurcation method [15], which avoids an explicit solving of the Stefan-Maxwell relationships.

The preceding equations were discretized using a finite-volume technique, and the tridiagonal matrix resolution is performed with the help of the algorithm of Thomas [16]. Time integrations are performed with an implicit Newton-Raphson technique. This transient solver is used for the mere determination of the steady-state behavior. Convergence is usually much slower in low-velocity situations, due to the increasing importance of backward diffusional effects.

2.2 Kinetic mechanism

Since hydrocarbon pyrolysis is a submechanism of combustion mechanism, numerous kinetic databases developed for the modeling of flames have been compiled for the constitution of our dataset.

Various steps may be distinguished during propane pyrolysis :
(i) An initial homolytic decompositon of propane leading to light species such as methane and C2 up to C4 hydrocarbons ; (ii) Various recombination steps between C2,C3 and C4 species leading to the first aromatic compounds, such as benzene, toluene, naphthalene, etc ...; and (iii) Formation of Polycyclic Aromatic Hydrocarbons (PAHs) by further addition or condensation mechanisms.

For the first steps of propane decomposition, leading to small species (less than three carbon atoms), the databases of Tomlin [17], Dente and Ranzi [18], Tsang *et al.* [19–21] and Baulch *et al.* [22, 23] were used. For the formation of heavier species such as benzene, naphthalene, and henanthrene, works on propane flames and soot formation of Marinov *et al.* [24], Westmoreland [25], Dean [26], Hidaka [27], Frenklach [28], Miller *et al.* [29] and Côme *et al.* [30–33] were used.

The reverse kinetic constants have been computed from thermodynamic considerations. The standard reaction enthalpies were computed from JANAF tables [34] and data from Barin *et al.* and Marinov [24], or from Benson's group contribution method [35–37] when no data were available.

Many species and reactions from this reference dataset have been eliminated, leaving a partially reduced mechanism including 53 species (the heaviest being phenanthrene) and 209 reactions.

3 PROPANE PYROLYSIS : RESULTS AND DISCUSSIONS

3.1 Chemical model validation

For the validation of the chemical mechanisms, partial pressures of main species at the outlet of the furnace where compared to experimental IR absorption for two temperature set points (1073 K and 1273 K in a 0.1 m long hot zone). Various inflow velocities were used, leading to residence times ranging from 0.05 s to 4 s. Pure propane was used as precursor with a pressure of 2 kPa. Details of the experimental procedure and analysis results are given elsewhere [39].

The comparison between computations and experience is only semi-quantitative, since only relative absorption data were available from FTIR measurements. It is known that the absorption peak areas of each species depend linearly on their concentration, but unfortunately the molar extinction coefficient is not known for every species. Moreover, if the species concentration is not constant all along the furnace length, the linearity is not verified any more. Fortunately, most molecular species are in constant concentration past the hot zone, that is, along most of the optical path. Comparing the partial pressures computed at the outlet of the furnace and the relative FTIR peak areas seems then to be sound enough for most molecular species.

The plots of figure 1 a) to d) show the good qualitative agreement between computations and FTIR data. It is excellent for some species such as propane, acetylene, ethylene, butadiene, benzene, and naphthalene. Marked differences appear for methane at low residence times, as well as for allene and vinylacetylene at low temperatures, probably because one or several extra decomposition pathways were not taken into account. Despite such discrepancies, the fact that the agreement is good for relatively heavy species is an indication of the pertinence of the model.
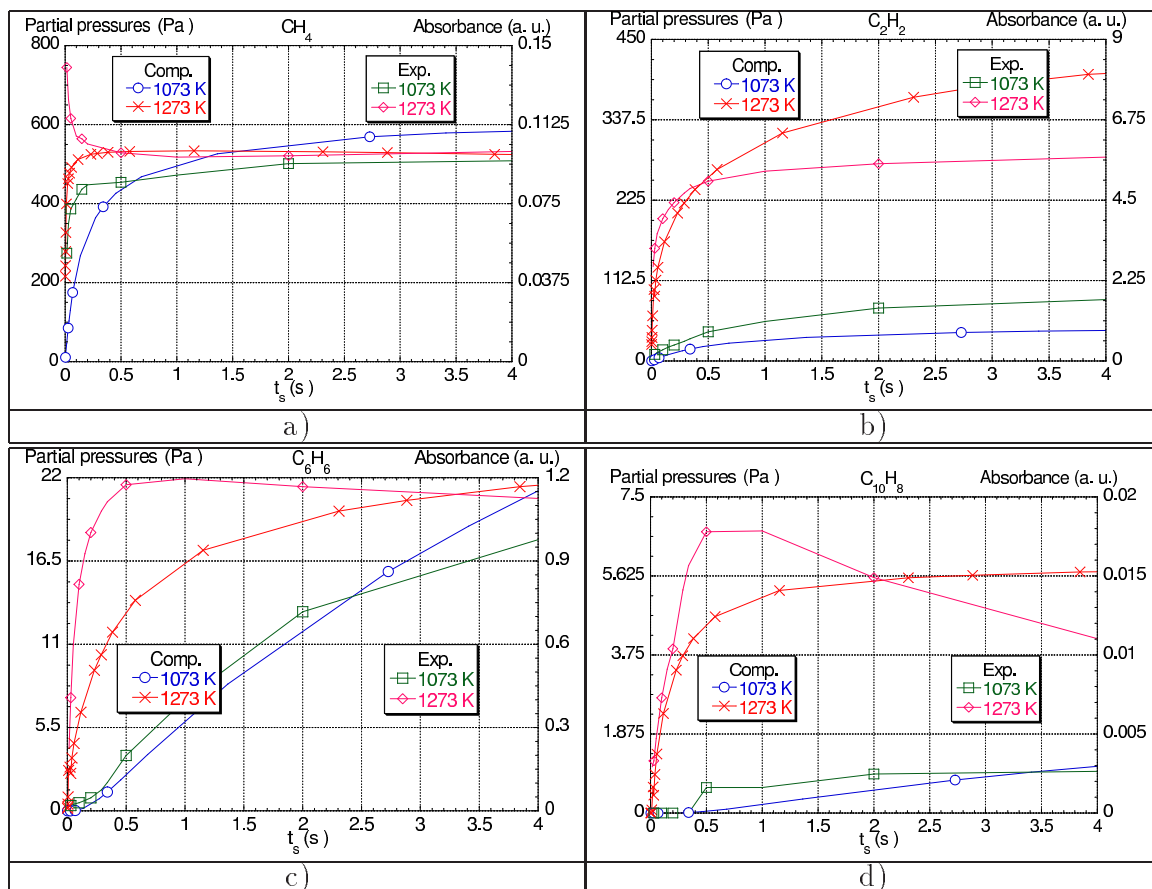
Figure 1. Computed species partial pressures *vs.* residence time at two temperatures. Comparison with FTIR data. Total pressure : 2 kPa. a) CH_4, b) C_2H_2, c) C_6H_6, d) $C_{10}H_8$.

3.2 Analysis of reaction fluxes

In order to have a synthetic viewpoint over the mechanisms of propane pyrolysis, an analysis of reaction fluxes has been carried out [14]. This allows to evidence the main reaction pathways for formation and decomposition of selected species of the kinetic model. The analysis has been performed at two reactor positions : $z = 0.4$ (beginning of the hot zone) and $z = 0.5$ (reactor center). This helps to understand the rôle of temperature and of the backward diffusion of the free radicals produced in the hottest zone. The main results are presented below.

Part 1 : Propane Decomposition. Propane is decomposed by metathesis evenly into 1-propyl and 2-propyl radicals. The unimolecular decomposition into C2+C1, which is one of the initial steps of the whole mechanism, is minoritary. On the other hand, at high temperatures, elimination of H_2 into propene dominates.

Ethylene originates itself essentially from two precursors : the propyl radical (predominantly at low temperatures), and the vinyl C_2H_3 radical. Ethylene gives back the vinyl in a reversible way, which limits the formation of acetylene from this radical. In the hot zone, the equilibrium is displaced towards vinyl and acetylene formation ; however, this mechanism for vinyl formation is less important than the decomposition of propene. These facts are coherent with the experimental observation that propene appears sooner (lower T and t_s) than ethylene. The methyl radicals also are due to 1-propyl decomposition, and yield equally methane and ethane.

While at the beginning of the hot zone acetylene leads to the propenyl radical $v - C_3H_5$, it rather participates to the formation of cyclic compounds (C_6H_6, C_6H_5) and PAHs (through the HACA mechanism, see later) at the reactor center.

Part 2 : The C3 submechanism. In this part of the mechanism, the propargyl radical C_3H_3 plays a central rôle[29, 40, 41]. It originates itself from allene and propyne, themselves produced by two ways : one from propenyl, and the other from ethynyl C_2H. As seen before, the propenyl does not come from dehydrogenation of propene, but rather from methyl addition on acetylene. On the other hand, C_2H also does not come from the dehydrogenation of acetylene, but rather from the decomposition of $n - C_4H_3$.

In the cold zone, the propenyl pathway is majoritary, but in the hot zone the C_2H way predominates because of the larger amounts of C4 compounds production.

The C3 submechanism is limited to an equilibrium between C_3H_3 and C_3H_4 in the cold zone, while in the hot zone, the production of benzene and C_5H_5 from C_3H_3 is active. This is in accordance with the experimental fact that C3 species appear for lower temperatures and residence times than C4 species.

Part 3 : C4 compounds. In this part, the key species is the resonance stabilized $i - C_4H_5$ radical[25, 42–44], which is able to feed both the direct formation of benzene by addition on acetylene, and the formation of propargyl. It originates itself principally from two sources : on one side, the dimerization of vinyl, and on another side the dehydrogenation of butadiene, itself produced by an addition of vinyl on ethylene. It essentially decomposes itself into vinylacetylene C_4H_4, which is (mainly in the hot zone) a source of C_2H radicals. In lesser amounts, it also leads to benzene by acetylene addition. Accordingly, it is deduced from these facts that benzene formation is owed principally to a C4 mechanism at low temperatures, but that the C3 pathway becomes non negligible at high temperatures.

Part 4 : Formation of aromatic compounds. Following various authors, benzene may be formed through two different pathways :
— The HACA mechanism (*H*ydrogen *A*bstraction, C_2H_2 *A*ddition) [28], which is an alternated succession of dehydrogenations and acetylene additions ;
— The RSFR mechanism (*R*esonance *S*tabilized *F*ree *R*adicals) [24, 45, 46], involving the addition of radicals like propargyl C_3H_3, methylallenyl/1,3-butadienyl C_4H_5 and cyclopentadienyl C_5H_5.

The results of the analysis show that : (*i*) benzene is not the only source for the PAHs ; for instance, naphthalene is quite exclusively produced by the dimerization of cyclopentadienyl. (*ii*) the HACA mechanism seems to be the main route to the formation of species with 3 or more cycles.

To conclude with this mechanism description, figs. 2 a) and b) summarize the main pathways, either at low temperature and residence time, or at high values for these parameters, that is, at low and high maturation conditions.

4   CORRELATION WITH PYROCARBON DEPOSITION

Féron [4] and Lavenac [39, 47] have determined deposition rates as a function of residence time in the same reactor that has been used for the FTIR study. Figure 3 a) gives typical results. Four domains may be distinguished :
1. A domain at low residence times ($t_s < 0, 1\ s$), for which the deposition rate increases with residence time, the limiting phenomenon is the rate of homogeneous reactions,
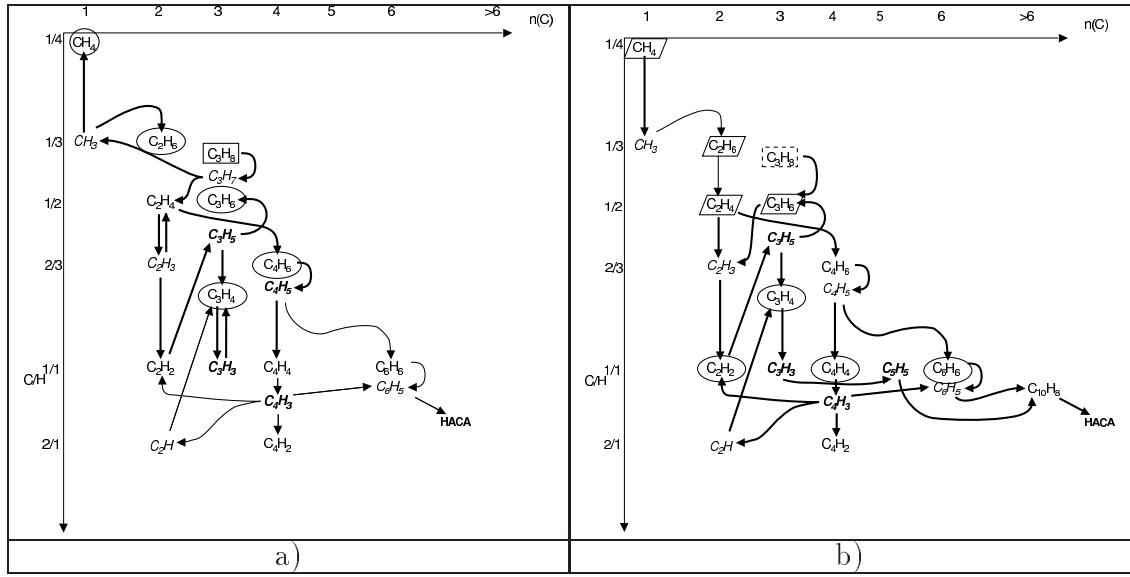
Figure 2. Main reaction pathways at a) low and b) high maturation conditions.

2. A plateau for which the surface reactions limit the total deposition rate,
3. A third domain for which the deposition rate increases strongly with residence time; homogeneous reactions are limiting.
4. A fourth domain with a decrease of the deposition rate, due to mass transfer limitations.
   It has also been found that smooth laminar (SL) pyrocarbon deposition coincides with the first
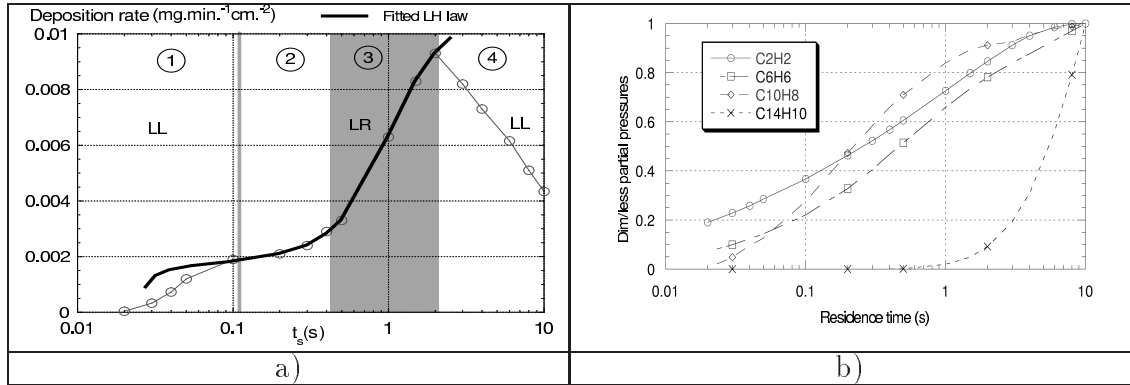
Figure 3. a) Mass deposition rate *vs.* residence time at $T = 1273$ K and $P = 2$ kPa. b) Dimensionless concentration profiles of some species *vs.* residence time in the same conditions.

two domains,whereas rough laminar (RL) pyrocarbon deposition occurs in the third domain, and the fourth domain corresponds again to SL. These results, in addition with those of kinetic study and gas-phase analysis by FTIR, have led to the following qualitative mechanism [4]:
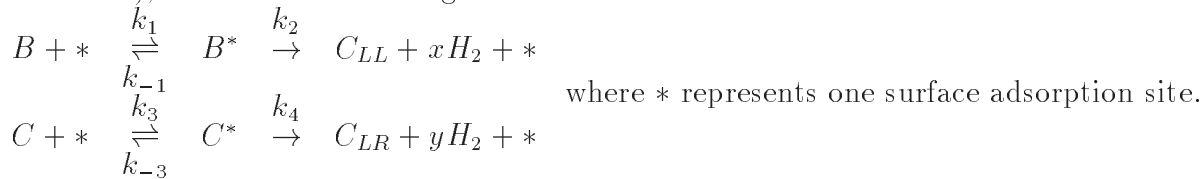
$$A \longrightarrow B \longrightarrow C$$
$$\downarrow \qquad \downarrow$$
$$SL \qquad RL$$
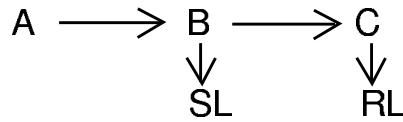
where A is the initial precursor, B stands for a group of light compounds and C stands for a group of heavier hydrocarbons ,which appear later during propane pyrolysis.

Since the studied reactor has a small surface-to-volume ratio, it may be considered in a first approximation that heterogeneous consumption reactions do not alter deeply the gas-phase concentrations of the reactants. In such a frame, one may try to correlate directly the deposition rates and nanostructures to the previously computed gas-phase concentrations. The most frequently cited species as precursors for pyrocarbon or soot formation are acetylene, benzene, and the PAHs. Accordingly, we have selected the two former, plus naphthalene and phenanthrene, which are the first PAHs that are included in model C, for a comparison with deposition rates. Figure 3 b) is a plot of their scaled concentrations in the hot zone *vs.* residence time. Comparison with figure 3 a) induces to separate the selected species into two groups, the first one comprising acetylene, benzene and naphthalene, which display a very analogous behavior (even if naphthalene looks to appear for

somewhat larger residence times), and the second one containing phenanthrene and whatever heavier species not taken explicitly into account in this model. The second group may be clearly related to the deposition of rough laminar pyrocarbon, and consequently the first one to smooth laminar pyrocarbon deposition.

The simplest attempt to build a quantitative model explaining pyrocarbon deposition would then be to select a species from group 1 (e. g. benzene) and another from group 2 (phenanthrene and PAHs), and construct a Langmuir-Hinshelwood mechanism :

$$B + * \underset{k_{-1}}{\overset{k_1}{\rightleftharpoons}} B^* \overset{k_2}{\to} C_{LL} + xH_2 + *$$

$$C + * \underset{k_{-3}}{\overset{k_3}{\rightleftharpoons}} C^* \overset{k_4}{\to} C_{LR} + yH_2 + *$$

where $*$ represents one surface adsorption site.

The kinetic law arising from such a mechanism has been fitted to the experimental data, and an excellent agreement has been found for the deposition domains 2 and 3, as shown in figure 3 a). The exact values of the correlation parameters are not of direct physical significance. However, some ratios allow to compare the two deposition mechanisms :
— The relative amount of adsorbed molecules for group B ($[B*]/[B]$) is much smaller than for group C. Three explanations for this are possible : (i) the light species adsorb less efficiently than the heavy ones, (ii) they desorb more easily, and (iii) they react faster when adsorbed. It is difficult to confirm one or another explanation since we do not have access to the adsorption constants.
— The group C incorporation reaction is just a little faster (in mole units) than for group B.

The transition from smooth laminar to rough laminar may thus be explained : at low residence times, there is a negligible amount of group C species, and the relatively slow mechanism yielding SL pyrocarbon dominates. The apparent order goes to zero when the surface sites are saturated with B^*, and this explains the plateau in zone 2. Note that it is not necessary to take into account the presence of hydrogen to explain the plateau. Then, for a higher gas-phase maturation, the faster RL deposition mechanism becomes predominant.

On the other hand, this model does not reproduce correctly the decrease of the deposition rate with residence time in the fourth zone ($t_s > 2$ s), but in this region, gas-phase transport limitations are such that the hypothesis of a weak coupling between heterogeneous reactions and gas-phase concentration fails.

5   CONCLUSION

In this work, a kinetic study for the pyrolysis of propane at 1100 and 1300 K and 2 kPa has been performed. A numerical model has been proposed, with a chemical mechanism including many light species and the first PAHs. It has been qualitatively validated with experimental in situ FTIR data, and partially reduced. Two kinds of results have been obtained.

First, reaction pathways have been elucidated, at least partially. The main conclusions are that :
— The propane decomposes into C2 species according to two mechanisms : a slow initiation step, and a radical metathesis main step,
— The C4 submechanism is more important than the C3 submechanism for benzene formation in the considered conditions,
— Benzene is not the only key species for PAH formation, there is also for example naphthalene which is obtained through a C3→C5 pathway,
— PAH growth occurs essentially through the HACA mechanism, except for some light aromatic compounds, such as naphthalene.

Second, a correlation has been carried out with deposition rate and nanostructure (SL/RL) data. It has been found that the heaviest species included in the model (and probably yet heavier ones) are crucial for the deposition of the RL form of pyrocarbon. On the other hand, benzene and acetylene seem to be more related to the formation of SL pyrocarbon. This does not exclude that they also play a rôle in RL formation.

The presented results are still limited to a particular experimental setup : it is intended in future work to apply the model to other situations, and to study the influence of other processing parameters such as temperature, precursor composition, and surface-to-volume ratio.

The reduction of the homogeneous mechanism has been only partially carried out, since it was already enough for a 1D solver ; it should be pushed forward by the application of more sophisticated methods, in order to use it in a 2D solver for CVI problems [48].
Also, more precise models should be sought for the heterogeneous chemistry part, as has been already made for diamond deposition [49], but a serious drawback is the almost complete lack of information about the structure of pyrocarbon surfaces : site abundances, defect distributions, etc. . . .

References

[1] Bokros, J.C., Deposition, structure and properties of pyrolytic carbon (M. Dekker, New York, 1969) pp. 1–118.

[2] Loll, P., Préparation et propriétés physiques de composites carbone/carbone déposés en phase vapeur (PhD thesis, Université Bordeaux 1, 1976).

[3] Loll, P., Delhaès, P., Pacault, A., and Pierre, A. *Carbon*, **15** (1977), 383-389.

[4] Féron, O., *CVD−CVI du pyrocarbone. Analyse in−situ de la phase gazeuse. Etudes cinétique et structurale.* (PhD thesis, Université Bordeaux I, 1998).

[5] Lieberman, M.L. and Pierson, H.O., *Carbon*, **12** (1974) 233-235.

[6] Pierson, H.O. and Lieberman, M.L., *Carbon*, **13** (1975) 159–166.

[7] McAllister, P. and Wolf, E.E., *AICHE J.*, **39** (1993) 1196–1209.

[8] Dupel, P., Pailler, R., and Langlais, F., *J. Mater. Sci.*, **29** (1994) 1341–1347.

[9] Féron, O., Langlais, F., Naslain, R., and Thébault, J., *Carbon*, **37** (1999) 1343–1353.

[10] Benzinger, W., Becker, A., and Hüttinger, K. J., *Carbon*, **34** (1996) 957–966.

[11] Becker, A. and Hüttinger, K.J., *Carbon*, **36** (1998) 177–199, **36** (1998) 201–211, **36** (1998) 213–224, **36** (1998) 225–232.

[12] Brüggert, M., Hu, Z., and Hüttinger, K.J., *Carbon*, **37** (1999) 2021–2030.

[13] Antes, J., Hu, Z., Zhang, W., and Hüttinger, K.J., *Carbon*, **37** (1999) 2031–2039.

[14] Descamps, C., Modélisation de l'infiltration chimique en phase vapeur isobare (I-CVI). Application au *SiC* et au pyrocarbone. (Ph. D. Thesis, Université Bordeaux 1, 1999).

[15] Bartlett, E.P., Kendall, R. M., and Rindal, R., (Technical Report 66-7, NASA, 1968).

[16] Press, W.H., Teukolsky, S. A., Vetterling, W. T., and Flannery, B. P., *Numerical recipes in FORTRAN. The art of scientific computing.* (Cambridge University Press, New York, 1992).

[17] Tomlin, A.S., Pilling, M. J., Merckin, J. H., Brindley, J., Burgess, N., and Gough, A., *Ind. Eng. Chem. Res.*, **34** (1995) 3749–3762.

[18] Dente, M.E. and Ranzi, E.M., "Mathematical modeling of hydrocarbon pyrolysis reactions", *Pyrolysis: Theory and industrial practice*, edited by L.F. Albright, B.L. Cranes, and W.H. Corcoran, (Academic press Inc., New York, 1983), pp. 133-151.

[19] Tsang, W., *Ind. Eng. Chem. Res.*, **31** (1992), 3–92.

[20] Tsang, W. and Hampson, R.F., *J. Phys. Chem. Ref. Data*, **15** (1986) 1087–1144.

[21] Tsang, W., *J. Phys. Chem. Ref. Data*, **16** (1987) 471–502, **17** (1988), 887–915, **20** (1991) 221–283.

[22] Baulch, D.L., Cobos, C.J., Cox, R.A., Esser, C., Frank, P., Just, T., Kerr ,J.A., Pilling, M.J., Troe, J., Walker, R.W., and Warnatz, J., *J. Phys. Chem. Ref. Data*, **21** (1992) 411–453 .

[23] Baulch, D.L., Cobos, C.J., Cox, R.A., Frank, P., Hayman, G., Just, T., Kerr ,J.A., Murrels, T., Pilling, M.J., Troe, J., Walker, R.W., and Warnatz, J., *Combustion and flame*, **98** (1994) 59–74.

[24] Marinov, N.M., Pitz, W.J., Westbrook, C.K., Castaldi, M.J., and Senkan, S.M., *Combust. Sci. and Tech.*, **116-117** (1996) 211–252.

[25] Westmoreland, P.R. and Howard, J.B., "Carbon formation from acetylene", Twenty first symposium on combustion, Munich, W. Germany, 1986, edited by (The Combustion Insitute,Pittsburgh, 1986) pp. 773-779.

[26] A. M. Dean, *J. Phys. Chem.*, **89** (1985) 4600–4618.

[27] Hidaka, Y., Hattori, K., Okuno, T., Inami, K., Abe, T., and Koike, T., *Combustion and Flame*, **107** (1996) 401–421.

[28] Frenklach, M. and Warnatz, J., *Combust. Sci. and Tech.*, **51** (1987)265–283.

[29] Miller, J.A. and Melius, C.F., *Combustion and Flame*, **91** (1992) 21–42.

[30] Barbé, P., Battin-Leclerc, F., and Côme, G.-M., *J. Chem. Phys.*, **92** (1995)1666–1685 .

[31] Côme, G.-M., Warth, V.F., Glaude, P.A.,Fournet, R., Battin-Leclerc, F., and Scacchi, G., "Computer-aided design of gas-phase oxidation mechanism : application to the modelling of normal heptane and iso-octane oxidation", 26th Intl. Symposium on Combustion, Naples, Italy, 1996, edited by A.R. Burgess, F.L. Dryer and N. Peters (The Combustion Institute, Pittsburgh, 1996).

[32] R. Fournet. Personal Communication, 1996.

[33] Fournet, R., Baugé, J.-C., and Battin-Leclerc, F., *Int. J. Chem. Kinetics*, **31** (1996) 361–390 .

[34] Chase Jr., M.W., Davies, C.A., Downey Jr., J.R., Frurip, D.J., McDonald, R.A., Syverud, A.N., editors, JANAF Thermochemical Tables, *J. Phys. Chem. Ref. Data* **14**(1985).

[35] Benson, S.W., Thermochemical kinetics (John Wiley & Sons, New York, 1976).

[36] Benson, S.W., Cruickshank, F.R., Golden, D.M., Haugen, G.R., O'Neal, H.E., Rodgers, A.S., Shaw, R., and Walsh, R. *Chem. Rev.*, **69** (1968) 279–298.

[37] Côme, G.-M., Réactions chimiques en phase gazeuse. Thermodynamique, cinétique, mécanismes réactionnels (Ellipses, Paris, 1999).

[38] Turányi, T., *New J. Chem.*, **14** (1990) 795–824.

[39] Lavenac, J., CVD du pyrocarbone laminaire ex-propane. Processus chimiques homogènes et hétérogènes, nanostructure. (PhD thesis, Université Bordeaux 1, 2000).

[40] Wu, C.H. and Kern, R.D., *J. Phys. Chem.*, **91** (1987) 6291–6307.

[41] Senkan, S. and Castaldi, M., *Combustion and Flame*, **107** (1996) 141–173.

[42] Cole, J.A., Bittner, J.D., Longwell, J.P., and Howard, J.B., *Combustion and Flame*, **56** (1984) 51–59.

[43] Stehling, F.C., Frazee, J.D., and Anderson, R.C., "Carbon formation from acetylene", Sixth Intl. Symposium on Combustion, Naples, Italy, (The Combustion Institute, Pittsburgh, 1956), pp. 247–253.

[44] Frenklach, M., "On surface growth mechanism of soot particles", 26th Intl. Symposium on Combustion, Naples, Italy, 1996, edited by A.R. Burgess, F.L. Dryer and N. Peters (The Combustion Institute, Pittsburgh, 1996) pp. 2285–2293.

[45] Melius, C.F., Coltrin, M.E., Marinov, N.M., Pitz, W. J., and Senkan, S.M., "Reaction mechanisms in aromatic hydrocarbon formation involving the C_5H_5 cyclopentadienyl moiety", 26th Intl. Symposium on Combustion, Naples, Italy, 1996, edited by A.R. Burgess, F.L. Dryer and N. Peters (The Combustion Institute, Pittsburgh, 1996) pp. 685–692.

[46] Emdee, J.L., Brezinsinky, K., and Glassman, I., "Oxidation of o-xylene", 23rd Intl. Symp. on Combustion, Orleans, France, 1990 (The Combustion Institute, Pittsburgh, 1990) pp. 77-85.

[47] Lavenac, J., Langlais, F., Féron, O., and Naslain, R., *to appear in Composites Science and Technology* (2000).

[48] Vignoles, G.L., Descamps, C., and Reuge, N., "Interaction between a reactive preform and the surrounding gas-phase during CVI", Euro-CVD 12, Barcelona, Spain, September 1999, edited by A. Figueras (volume 97-25 of *Journal de Physique*, EDP Sciences, Les Ulis, 1999) pp. Pr2-9.

[49] Okkerse, M., de Croon, M.H.J.M., Kleijn, C.R., van den Akker, H.E.A., and Marin, G.B., *J. Appl. Phys.*, **84** (1998) 6387–6398.